Biophysical Chemistry 26 (1987) 247–261
Elsevier

BPC 01143

Protein dynamics

A time-resolved fluorescence, energetic and molecular dynamics study of ribonuclease T_1

Alexander D. MacKerell Jr [a], Rudolf Rigler [a], Lennart Nilsson [a], Ulrich Hahn [b] and Wolfram Saenger [b]

[a] *Department of Medical Biophysics, Karolinska Institutet, S-104 01 Stockholm, Sweden and* [b] *Institute for Crystallography, Free University Berlin, Takustrasse 6, D-1000 Berlin 33, Germany*

Accepted 27 February 1987

Ribonuclease T_1; Protein dynamics; Time-resolved fluorescence; Thermodynamics; Molecular dynamics

Studies using time-resolved fluorescence depolarization were performed on the internal motion of Trp 59 of ribonuclease T_1 (EC 3.1.27.3) in the free enzyme, 2′-GMP-enzyme complex and 3′-GMP-enzyme complex. The Trp 59 motion was also studied in the free enzyme using molecular dynamics simulations. Energetic analysis of activation barriers to the Trp 59 motion was performed using both the transition state theory and Kramers' theory. The activation parameters showed a dependence on solvent viscosity indicating the transition state approach in aqueous solution to be inadequate. When taking solvent viscosity contributions into account agreement between the transition state and Kramers' theories was obtained. The results indicate the three enzyme forms to have different conformations with the free enzyme and 3′-GMP-enzyme complex being similar. Comparison of the experimental and theoretical results showed a good agreement on the Trp 59 motion in the free enzyme. Trp 59 appears to vibrate rapidly, with a relaxation time of the order of 1 ps, within free space in the protein matrix and to have a slower motion, with a relaxation time of the order of 100 ps, which is related to breathing of the surrounding protein matrix. Molecular dynamics results indicate high mobility in regions of the enzyme involved in the interaction with the guanine base of the inhibitor or substrate while much lower mobility occurred in residues involved in the catalytic mechanism of ribonuclease T_1.

1. Introduction

Enzyme dynamics have recently been the focus of study concerning their relation to functional aspects. Such studies have included both the theoretical approach of molecular dynamics simulations [1–3] and experimental techniques including X-ray temperature factors [4,5], NMR [6–8], time-resolved fluorescence spectroscopy [9–11] and flash photolysis [12], among others. Furthermore, the influence of the surrounding solvent on protein dynamics has also recently been emphasized [13].

Kramers [14] initially suggested the influence of Brownian motion on the crossing of a potential energy barrier in a chemical reaction. This approach has recently been applied to proteins in an attempt to understand the effect of the surrounding solvent on various proteins [13]. Reactions observed have included the movement of ligands through the protein matrix and the binding of ligands to the heme in hemoglobin and myoglobin [12,15] and the turnover rate of carboxypeptidase A [16]. In these studies the solvent viscosity was assumed to exert the largest effect on the observed

Dedicated to Professor Manfred Eigen on the occasion of his 60th birthday.

Correspondence address: R. Rigler, Department of Medical Biophysics, Karolinska Institutet, S-104 01 Stockholm, Sweden.

reaction rates, following the assumption that protein dynamics dictated the reaction being observed. The motion of a tryptophan residue within a protein, as monitored by time-resolved fluorescence depolarization measurements [17], offers a direct means to study the effect of solvent viscosity on protein dynamics.

Time-resolved fluorescence depolarization measurements, due to recent advances in single photon counting techniques [18,19], allows motions occurring in the time range of picoseconds to nanoseconds to be observed. The direct relationship between the correlation function and the measurement allows direct interpretation of the results as compared to NMR [20]. Furthermore, the presence of the intrinsic chromophore, tryptophan, in a variety of proteins makes the method widely applicable. Problems, however, can arise due to complexities in the photophysics of tryptophan [21,22]. Thus, it is advantageous to apply the technique to single-tryptophan-containing proteins, such as ribonuclease T_1 [23–27], to minimize difficulties in data interpretation.

Understanding of the dynamics of proteins has been greatly accelerated by the use of computer simulations [1–3]. Results from these molecular dynamics studies have shown reasonable agreement with experimental data, including X-ray temperature factors [5,28]. Several molecular dynamics studies have examined the motion of protein aromatic residues; the tyrosines in bovine pancreatic trypsin inhibitor [29,30] and the tryptophans in lysozyme [31]. In both studies, however, direct correlation between simulation and experimental results was lacking.

Ribonuclease T_1 (RNase T_1; EC 3.1.27.3), which has been crystallized in the presence of both 2′-GMP [32,33] and 3′-GMP [34], offers an ideal system for the study of protein dynamics. The enzyme specifically cleaves single-stranded RNA on the 3′ side of guanylic acid residues via a guanosine 2′,3′-phosphate intermediate which is hydrolyzed to yield a terminal 3′-guanylic acid [35–37]. Residues involved in the catalytic mechanism include His 40, Glu 58, Arg 77 and His 92. Significantly, the single tryptophan in the enzyme, Trp 59, is adjacent to the catalytic residue, Glu 58, in the primary sequence allowing the observation of motions adjacent to the active site of the enzyme.

Previously, we have shown the presence of a fast motion associated with Trp 59 using time-resolved fluorescence depolarization [38]. This motion, with a rotational correlation time in the range of 200 ps at 20 °C and of limited amplitude, was suggested to be associated with periodic motions of Trp 59 or with motional fluctuations of the region containing that residue. Furthermore, it was observed that both the rotational correlation time and the amplitude of the motion increased in the presence of the inhibitors 2′-GMP and 3′-GMP, indicating changes in the enzyme conformation. In this report we present results of a study on the energetic aspects, including solvent viscosity contributions, of the barrier to the fast motion of Trp 59 in the free enzyme, and the 2′-GMP-enzyme and 3′-GMP-enzyme complexes. Furthermore, results from a molecular dynamics simulation of the free enzyme are compared with and used to aid in the interpretation of the experimental results.

2. Materials and methods

2.1. Materials

Guanosine 2′-monophosphate (disodium salt), guanosine 3′-monophosphate (trisodium salt) and *N*-acetyl-L-tryptophanamide were obtained from Sigma, St. Louis. Glycerol, fluorescence microscopy grade, was from Merck. All other chemicals were reagent grade. Water was treated by ion exchange, then distilled and lastly distilled against alkaline potassium permanganate prior to use.

2.2. Methods

RNase T_1 was purified from *Aspergillus oryzae* extract following a procedure similar to that of Rüterjans and Pongs [39]. The purified enzyme was the p*I* 3.0 isozyme, where Gln 25 is exchanged with Lys [32]. Following purification the enzyme was lyophilized for storage and then redissolved in distilled water prior to use. Enzyme concentrations were 10 μM and were determined

by absorption at 278 nm in 50 mM phosphate (pH 7.0) using an extinction coefficient of 2.12×10^4 M^{-1} cm^{-1} [37] on a Cary 118 sepctrophotometer.

Fluorescence titrations and time-resolved experiments were performed in 50 mM sodium acetate (pH 5.3), containing 0.1 mM EDTA or in buffer/glycerol mixtures. Buffer/glycerol mixtures were prepared by mixing the pH 5.3 acetate buffer with various volumes of glycerol to obtain solutions of 3.3–38.8% (w/w) glycerol. The percent glycerol in the solutions for the constant-viscosity measurements was chosen to maintain a viscosity of 2 cP at the various temperatures [40]. For the varied-viscosity (isothermal) condition measurements solutions of 0–40% (w/w) glycerol were prepared to obtain viscosities of 1.0–5.6 cP at 20°C (see fig. 3). Temperature regulation (±0.1°C) was performed using a Lauda circulating bath.

Fluorescence titrations of RNase T_1 with 2′-GMP and 3′-GMP were performed on a Shimadzu RF-540 spectrofluorophotometer using an excitation wavelength of 300 nm (band width: 5 nm) and an emission wavelength of 380 nm (band width: 30 nm). Fluorescence intensity was followed while adding aliquots of the inhibitor and maintaining the enzyme concentration. Association constants, K_a, were determined using

$$K_a = \frac{EI_i}{E_i I_i} \tag{1}$$

where E_i, I_i and EI_i are the respective concentrations of free enzyme, unbound inhibitor and enzyme-inhibitor complex at titration point i. EI_i was assumed to be proportional to the amount of fluorescence quenching and to be equal to the total enzyme concentration when maximum quenching, indicating saturation of the enzyme by the inhibitor, was obtained.

Time-resolved fluorescence measurements were performed using time-correlated single-photon counting as previously described [18,19,41,42]. Experiments were performed at an excitation wavelength of 300 nm and emission was monitored through a WG 360 nm cutoff filter. Data collection involved four groups of 2048 channels each and included the excitation pulse, unpolarized (magic angle) fluorescence, dark current and perpendicularly polarized fluorescence. Individual experiments contained up to 2×10^5 counts per channel [38]. Data, due to background fluorescence from the inhibitors (10% or less of enzyme-inhibitor counting rate), were subjected to a background subtraction procedure as described previously [38].

Data analysis, including convolution of the excitation pulse with the physical models [43], has been previously described [42]. Fluorescence decays, $I_m(t)$, were treated as a sum of individual fluorescence lifetimes according to:

$$I_m(t) = \sum_j a_j \exp\left(-t/\tau_j\right) \tag{2}$$

where τ_j is the fluorescence decay lifetime and a_j the respective amplitude. Anisotropic decays, $r(t)$, were calculated from the measured unpolarized, $I_m(t)$, and perpendicularly polarized, $I_\perp(t)$, fluorescent components using:

$$r(t) = 1 - I_\perp(t)/A(I_m(t)) \tag{3}$$

where A is a correction factor to compensate for the difference in detector sensitivity to the unpolarized, $I_m(t)$, and perpendicularly polarized, $I_\perp(t)$, components and equals 1.05 in this study. Rotational relaxation times, due to the anisotropy being a function of both the rotational relaxation times and the fluorescence decay times [44–46], were fitted by assuming that each rotational relaxation is associated with all the fluorescence decays:

$$\frac{I_\perp(t)}{I_m(t)} = 1 - \frac{\left(\sum_i r_{oi} \exp(-t/\theta_i)\right)\left(\sum_j a_j \exp(-t/\tau_j)\right)}{\sum_j a_j \exp(-t/\tau_j)} \tag{4}$$

where r_{oi} is the zero-time anisotropy for i, θ_i the rotational relaxation time for i, a_j the amplitude of fluorescence decay j and τ_j the fluorescence decay time for j. This model is well suited for a single-tryptophan protein where the fluorescence

from the tryptophan should be associated with both overall rotation of the enzyme and internal motions of the tryptophan itself.

The technique used for the measurement of time-resolved fluorescence depolarization decays has recently been improved to allow the observation of rotational motions into the picosecond time range [18,19]. Inherent in the system, due to the alternating measurement of the instrument response, magic angle, dark current and perpendicular angle is a 'self-calibration' which helps to compensate for drift in the excitation source and detection electronics. Limitations, however, do exist including the detection channel width and the amount of sample counts per channel that can be collected which limit the statistical significance one may obtain using this technique. To overcome these problems measurements being directly compared were made in the same experimental session, such that the sequence of measurements in aqueous solution (see fig. 1) at 4, 20 and 40 °C and 12 and 30 °C were performed consecutively as were measurements under the isoviscosity (see fig. 2) and isothermal (see fig. 3) conditions. Furthermore, to eliminate potential problems due to photodegradation, although such effects have previously been shown to be insignificant [23,47], fresh enzyme samples were used for each measurement.

A molecular dynamics simulation of the free enzyme was performed using the CHARMM program [48]. The initial coordinates were those for the 2′GMP-enzyme complex at pH 5.5 [32] with the 2′-GMP removed. The system included 949 atoms (779 protein nonhydrogen atoms and 170 polar hydrogen atoms) and used the current CHARMM parametrization for all energy interactions. Prior to the actual trajectory the system was energy minimized using the Adopted Basis Newton-Raphson algorithm for 200 steps followed by heating from 0 to 313 K in 2.0 ps and equilibration for an additional 20 ps, using a step size of 0.001 ps. Following the equilibration the trajectory used in the analysis was continued for 55.5 ps. Using a MicroVAX II computer 1 ps of simulation time required 10 central processor unit (CPU) hours.

Comparison of results from the molecular dynamics trajectory with the experimental results on the tryptophan motion requires the calculation of the correlation function, P_2, between the absorption, $\hat{\mu}_a$, and emission, $\hat{\mu}_e$, vectors of tryptophan using:

$$r(t) = 0.4(\exp(-t/\theta_m))\langle P_2[\hat{\mu}_a(0)\cdot\hat{\mu}_e(t)]\rangle \quad (5)$$

where $r(t)$ is the anisotropy as a function of time, θ_m the rotational relaxation time for the overall rotation of the protein and $P_2(x)$ the second-order Legendre polynomial [31]. We assume two rotational relaxations to be present due to internal motions of Trp 59 ($\theta_1 \ll \theta_2 \ll \theta_m$) which relax to plateau values of P_∞^i such that:

$$\langle P_2[\hat{\mu}_a(0)\cdot\hat{\mu}_e(t)]\rangle = \left[\left(1-P_\infty^1\right)e^{-t/\theta_1}+P_\infty^1\right] \times\left[\left(1-P_\infty^2\right)e^{-t/\theta_2}+P_\infty^2\right] \quad (6)$$

Combination of eqs. 5 and 6 yields:

$$r(t) = r_o\left[\left(1-P_\infty^1\right)e^{-t/\theta_1}+P_\infty^1\right] \times\left[\left(1-P_\infty^2\right)e^{-t/\theta_2}+P_\infty^2\right]e^{-t/\theta_m} \quad (7)$$

where r_o is related to the angle between the tryptophan absorption, $\hat{\mu}_a$, and emission, $\hat{\mu}_e$, vectors (see section 3). In the analysis of the molecular dynamics trajectory the exponential term containing θ_m is equal to unity, due to the overall rotation and translation of the protein not being present. The analysis of the experimental data (see eq. 4 and section 3) assumed the very fast rotational relaxation, θ_1, to be unobservable due to experimental limitations, yielding the equation:

$$r(t) = r_o P_\infty^1\left(1-P_\infty^2\right)e^{-t/\theta_2} + r_o P_\infty^1 P_\infty^2 e^{-t/\theta_m} \quad (8)$$

where there are two rotational relaxation times θ_2 and θ_m for the internal Trp 59 motion and the overall enzyme rotation, respectively, with the two assumed to be uncoupled. This assumption is valid while the fast and overall rotational correlation times differ by an order of magnitude or more. The value of the experimental total zero-time anisotropy, $r_{o,total}$, equals $r_o P_\infty^1$ in eq. 8 and the experimental zero-time anisotropy associated with the internal Trp 59 motion, r_{o2}, equals $r_o P_\infty^1(1-P_\infty^2)$ in eq. 8.

3. Results

3.1. Fluorescence titrations

Fluorescence titrations of RNase T_1 with 2′-GMP and 3′-GMP were performed to determine the respective association constants for the inhibitors. These experiments were performed under conditions similar to those used in the aqueous solution and isoviscosity time-resolved measurements. The results showed a tighter binding of 2′-GMP vs. 3′-GMP under the conditions used, in agreement with previous results [37]. For 2′-GMP association constants varied with increasing temperature from 1.8 to 0.4×10^6 M^{-1} in aqueous solution and from 1.0 to 0.7×10^6 M^{-1} under isoviscosity conditions. With 3′-GMP under aqueous conditions the association constant decreased from 4.0 to 1.0×10^5 M^{-1} as temperature increased and from 3.0 to 1.0×10^5 M^{-1} under isoviscosity conditions. These values where then used to determine the inhibitor concentration for the time-resolved experiments at which a minimum of 93% saturation occurred.

3.2. Time-resolved fluorescence measurements

The fluorescence decay times (τ_j) and percentage weights (w_j) in aqueous solution at pH 5.3 and 40 °C are listed in table 1. Examination of the results for the free enzyme shows the presence of two decay times with the shorter decay time, τ_3, being the minor component. With the 2′-GMP-enzyme complex three times are present, a very fast component, τ_2, and two longer decay times, τ_3 and τ_4, with the longer of the two being the minor component. Four components are observed in the 3′-GMP-enzyme, two very fast components, τ_1 and τ_2, and two longer components, τ_3 and τ_4, with the τ_3 component being the minor component, similar to that observed in the free enzyme.

Table 1

Fluorescence decay and rotational relaxation parameters for ribonuclease T_1

Values reported for 40 ° C in aqueous solution (see section 2). τ (ns), fluorescence decay time; a, amplitude; θ, rotational relaxation times; r_o, zero-time anisotropy.

	Free enzyme	2′-GMP-enzyme	3′-GMP-enzyme
Fluorescence decays			
$\tau_1(a_1)$			0.01 (43%)
$\tau_2(a_2)$		0.01 (79%)	0.04 (39%)
$\tau_3(a_3)$	1.81 (17%)	2.24 (13%)	1.91 (2%)
$\tau_4(a_4)$	3.69 (83%)	3.41 (8%)	2.70 (16%)
χ^2	1.49	1.86	2.46
Rotational relaxation			
$\theta_2(r_{o,2})$	0.10 (0.044)	0.16 (0.048)	0.23 (0.061)
$\theta_m(r_{o,m})$	2.90 (0.220)	2.68 (0.185)	3.51 (0.200)
$r_{o,total}$	0.264	0.233	0.261
χ^2	1.11	1.12	1.42

Previous results with RNase T_1 (free enzyme) have varied as to the number of fluorescence decay components present [23–27]. To confirm the presence of the minor fluorescence component in the free enzyme (table 1) control measurements using *N*-acetyl-L-tryptophanamide (NATA) under similar experimental and instrumental conditions were performed and showed a single fluorescence decay time of 3.0 ns in agreement with previous results [22]. The fast fluorescence components in the enzyme-inhibitor complexes, due to the slight absorption at 300 nm by 2′-GMP [35], were suspected as possibly originating from the inhibitors alone. While contributions from the unbound inhibitors were corrected for by the subtraction procedure it must be emphasized that contributions to the fluorescence which we associate with Trp 59 may arise from the guanine base or Tyr 42 or Tyr 45, due to their involvement in a highly specific stacked configuration in the enzyme-inhibitor complexes [32–34].

3.3. Rotational energetic analysis

3.3.1. Measurements in aqueous solution

Traditional approaches to the analysis of potential energy barriers use the transition state theory [49], where the crossing of a barrier is assumed to be independent of the surrounding environment. In this approach the measured rate constant, $k(1/\theta_2)$, is determined as a function of temperature, T (K):

$$k = \nu \exp(-\Delta G^*/RT) \qquad (9)$$

where ν is the frequency factor, equaling 10^{13} s^{-1}, and R is the gas constant, allowing the energy of

the barrier, $\Delta G^{\neq}$, to be determined. From:

$$\Delta G^{\neq} = \Delta H^{\neq} - T\Delta S^{\neq} \quad (10)$$

the individual contributions of enthalpy, $\Delta H^{\neq}$, and entropy, $\Delta S^{\neq}$, were determined.

Initial analysis of the activation energy barrier to the motion of Trp 59 in RNase T_1 followed the approach presented in eqs. 9 and 10. In these experiments the rotational relaxation time, θ_2, associated with the internal motion of Trp 59 was measured at five different temperatures in aqueous buffer. The results, presented in fig. 1, show the temperature dependence for the free enzyme 2′-GMP-enzyme and 3′-GMP-enzyme. As may be seen, the free enzyme has the fastest rotational relaxation rate across the temperature range studied. Interestingly, the θ_2 values for the 2′-GMP-enzyme and 3′-GMP-enzyme cross, with the relaxation rate for the 3′-GMP-enzyme being faster at the lower temperature. This crossing effect, when considering the similar θ_2 values for the enzyme-inhibitor complexes at 20 °C, 0.25 and 0.23 ns for the 2′-GMP- and 3′-GMP-enzyme complexes at 20 °C, respectively [38], shows the importance of determining θ_2 at various temperatures to allow differences between the two enzyme-inhibitor complexes to be observed.

A quantitative evaluation of the results presented in fig. 1 is presented in table 2. In the analysis the frequency factor, ν, was assumed to be constant for all temperatures and enzyme forms studied. Inspection of the values in table 2 shows a similar enthalpic barrier for the free enzyme and the 2′-GMP-enzyme while a smaller enthalpic barrier occurs in the 3′-GMP-enzyme. Conversely, the most unfavorable (in terms of decreasing the rotational rate) entropic term occurs with the 3′-GMP-enzyme whereas the most favorable (in terms of increasing the rotation rate) term occurs with the free enzyme. Significantly, comparison between the three enzyme forms reveals that the longer rotational correlation time in the presence of inhibitors is due to an entropic effect, which is most pronounced in the 3′-GMP-enzyme. Furthermore, the different enthalpic values between the 2′-GMP-enzyme and 3′-GMP-enzyme lead to the crossing of the θ_2 values in fig. 1.

Table 2

Energetic activation parameters for the tryptophan motion in aqueous solution

Errors are of the order of 10%. Free energies are for 293 K. See section 2 for experimental conditions.

	Free enzyme	2′-GMP-enzyme	3′-GMP-enzyme
Enthalpy (kJ mol^{-1})	20.1	20.5	7.1
Entropy (J mol^{-1} K^{-1})	8.4	4.2	−40.1
Free energy (kJ mol^{-1})	17.6	19.3	18.8

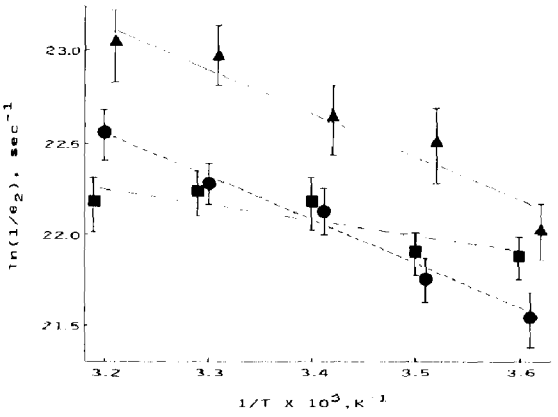

Fig. 1. Rotation rate vs. inverse temperature in aqueous solution for the free enzyme (▲), 2′-GMP-enzyme (●) and 3′-GMP-enzyme (■). Inhibitor concentrations were 30 and 60 μM for 2′-GMP and 60 and 100 μM for 3′-GMP at 4–20 and 30–40 °C, respectively.

3.3.2. *Isoviscosity measurements*

Analysis of activation energy barriers using the transition state theory ignores changes solvent properties that occur with temperature which may influence the reaction being observed. Thus, the energy parameters being measured will have contributions from both the protein itself and the surrounding solvent. One approach to eliminate the influence of solvent properties on the measured parameters is to perform the measurements at various temperatures while maintaining the solvent properties, thereby observing energy parameters from the protein alone [12]. Holding all solvent properties constant, however, is difficult, thus the property of viscosity, which should have the most direct effect on protein dynamics

[12,13], was chosen to be maintained while the temperature was varied.

The solvent viscosity was maintained by preparing different percent glycerol solutions for use at different temperatures (see section 2). The viscosity chosen, 2 cP, was selected to be similar to that of water and to keep the highest percent glycerol relatively low (less that 40%). By keeping the percent glycerol low changes in other solvent properties (ionic strength, pH) could be assumed to be negligible.

Fig. 2 shows the results from the constant-viscosity experiment for the three enzyme forms studied. Again, as in fig. 1, the free enzyme has the fastest rotational relaxation rate throughout the temperature range studied, while the values for the 2′-GMP-enzyme and 3′-GMP-enzyme again cross. In this case, however, the 2′-GMP-enzyme has the fastest rotational relaxation rate at the lowest temperature, a reversal of the effect observed in the experiments in aqueous solution (see above).

Evaluation of the results in fig. 2 was performed analogously to the aqueous experiments:

$$k = \nu \exp(-\Delta G^{**}/RT) \quad (11)$$

$$\Delta G^{**} = \Delta H^{**} - T\Delta S^{**} \quad (12)$$

with the asterisk indicating constant viscosity (isoviscosity). Calculated values from these measurements, where solvent viscosity contributions to the activation parameters are assumed to be negligible (i.e., protein alone), are presented in table 3. In contrast to the aqueous results (table 2), similar enthalpic contributions to the activation barrier occur in the free enzyme and 3′-GMP-enzyme while a lower value is found for the 2′-GMP-enzyme. Again, entropic effects, which are more unfavorable with the enzyme-inhibitor complexes, appear to cause the longer rotational relaxation times.

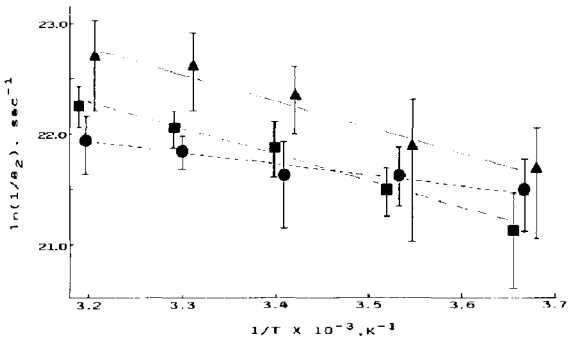

Fig. 2. Rotation rate vs. inverse temperature with viscosity held constant (isoviscosity) for the free enzyme (▲), 2′-GMP-enzyme (●) and 3′-GMP-enzyme (■). Inhibitor concentrations were 60 μM for 2′GMP at all temperatures and 120 and 140 μM for 3′-GMP at 0–10 and 20–40 °C, respectively.

Table 3

Energetic activation parameters for the tryptophan motion in isoviscosity

Errors are the order of 10%. Free energies are for 293 K. See section 2 for experimental conditions.

	Free enzyme	2′-GMP-enzyme	3′-GMP-enzyme
Enthalpy (kJ mol^{-1})	20.1	7.5	20.1
Entropy (J mol^{-1} K^{-1})	4.2	−42.6	0.0
Free energy (kJ mol^{-1})	18.9	20.0	20.1

3.3.3. *Isothermal measurements*

Contribution from the solvent may also be considered using Kramers' equation [12–14,16]:

$$k = (\nu_o \nu_o' \rho/3\eta) \exp(-\Delta G^{**}/RT) \quad (13)$$

where k is the measured reaction rate, ν_o the undamped frequency in the initial well (10^{13} s^{-1}), ν_o' the undamped frequency at the top of the activation energy barrier (10^{14} s^{-1}), ρ the linear mass density (10^{-14} g cm^{-1}) and ΔG^{**} the barrier height in the protein. In this approach the solvent viscosity, η, is of primary importance to the reaction rate. When dealing with the internal motions of proteins a factor κ is introduced into eq. 13 to account for the transmission of the viscosity by the protein matrix [12], yielding:

$$k = (A/3\eta^{\kappa}) \exp(-\Delta G^{**}/RT) \quad (14)$$

The influence of the solvent viscosity on the internal motion associated with Trp 59 was assessed by measuring the rotational relaxation time at various viscosities (1.0–5.6 cP) and constant temperature. The results from this experiment, plotted as ln k vs. ln η, are shown in fig. 3. Values of κ, de-

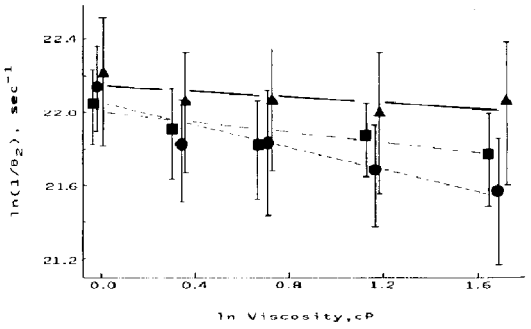

Fig. 3. Rotation rate vs. viscosity at constant temperature (20 °C, isothermal conditions) for the free enzyme (▲), 2′-GMP-enzyme (●) and 3′-GMP-enzyme (■). Inhibitor concentrations were 60 μM for 2′-GMP and 120 μM for 3′-GMP at all viscosities.

termined from the slopes in fig. 3, were 0.08, 0.31 and 0.14 for the free enzyme, 2′-GMP-enzyme and 3′-GMP-enzyme, respectively.

3.4. Zero-time anisotropy and overall rotational correlation time

The various time-resolved experiments also gave values for the overall rotational relaxation time and for the zero-time anisotropies, r_o (table 1). Results on the overall rotational relaxation time, θ_m, agreed with values calculated from the Stokes-Einstein relationship for a spherical molecule the size of RNase T_1 [32] when taking into account the viscosity and temperature. For the zero-time anisotropies associated with the fast rotational relaxation time, r_{o2}, the average values were 0.027 ± 0.011, 0.037 ± 0.012 and 0.045 ± 0.013 for the free enzyme, 2′-GMP-enzyme and 3′-GMP-enzyme, respectively. Average values for the total zero-time anisotropy, $r_{o,total}$, were 0.259 ± 0.014, 0.253 ± 0.013 and 0.251 ± 0.012 for the free enzyme, 2′-GMP-enzyme and 3′-GMP enzyme, respectively. From the values of r_{o2} and $r_{o,total}$ the angle of the fast motion, ω_f, can be determined using [8]:

$$\omega_f = \cos^{-1}\left(1/2\left((1+8S)^{1/2}-1\right)\right) \quad (15)$$

$$S^2 = (r_{o,total} - r_{o2})/r_{o,total} \quad (15a)$$

which models the motion as diffusion within a cone of semiangle ω_f. The resulting values were 15.5, 18.5 and 20.6° for the free enzyme, 2′-GMP-enzyme and 3′-GMP-enzyme, respectively.

3.5. Molecular dynamics simulation

Molecular dynamics studies were performed on the free enzyme due to the experimentally measured rotation of Trp 59 being fastest in that enzyme form. During the equilibration period (20 ps) a decrease in potential energy of the enzyme occurred, apparently due to conformational changes in the enzyme (MacKerell et al., manuscript in preparation). Once the potential

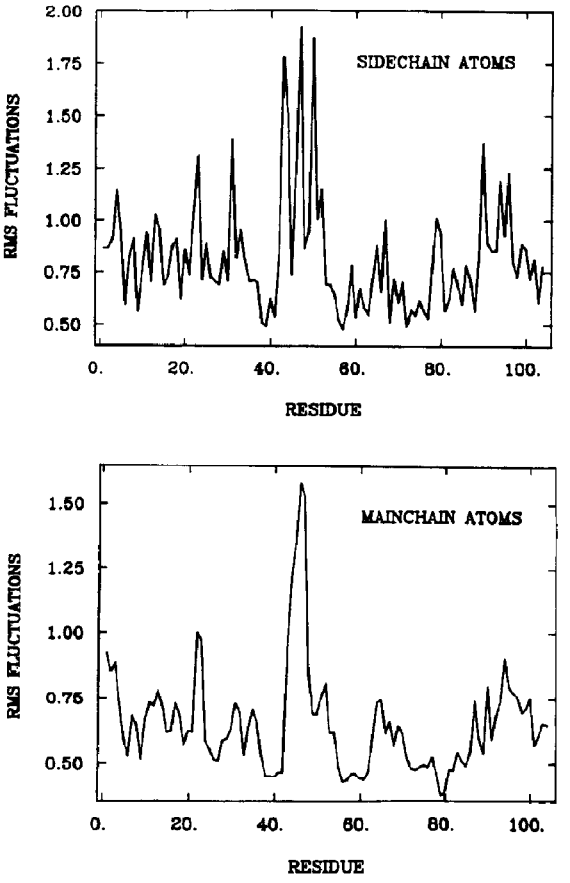

Fig. 4. Root mean square fluctuations (in Å) for the side chain (upper panel, excluding hydrogens and using Gly O) and the main chain (lower panel, N, Cα, C, O) atoms of ribonuclease T_1 from the molecular dynamics simulation of the free enzyme.

energy became constant the system was assumed to be at equilibrium. The conformational relaxation of the enzyme apparently also leads to an increase in the temperature of the system to an average of 324 K for the trajectory.

Analysis of the molecular dynamics trajectory emphasized overall root mean square motions of the enzyme and motion related to Trp 59. Root mean square fluctuations of the enzyme by residue for the main chain and side chain atoms are presented in fig. 4. Regions of large motion include the amino-terminus, residues 22 and 23, 43–50 and 93–96. Three regions of low mobility are noticeably present: residues 38–43, 56–62 and 77–81. Correlations between the absorption and emission vectors of Trp 59 were determined to study the motion of Trp 59. To calculate the correct cross-correlation function, P_2 (see section 2) the intrinsic angle, λ, between the tryptophan absorption and emission vectors must be used. Steady-state polarization studies on indole have indicated a zero-time anisotropy of approx. 0.31 with excitation at 300 nm [50]. Taking this value and using [31]:

$$r_o/0.4 \cong P_2(\cos\lambda) = (3\cos^2\lambda - 1)/2 \qquad (16)$$

a λ value of $\pm 23°$ is calculated ($P_2 = 0.77$). Excitation at 300 nm primarily excites the ^1L_a excitation band [50] which has an orientation of $-38°$ to the long axis of the tryptophan side chain [51]. Using this value for the ^1L_a ($\hat{\mu}_a$) absorption band, values of -15 and $-61°$ for the emission vector ($\hat{\mu}_e$) were determined. A plot of P_2 vs. time for both the -15 and $-61°$ emission vectors is presented in fig. 5. As may be seen in both the -15 and $-61°$ cases the correlation function quickly decreases within 1 ps to a value of 0.61, corresponding to a relaxation time of approx. 1 ps and an r_o of 0.24. Following the very fast decay the P_2 value remained constant in the case of the $-15°$ emission vector while a gradual decrease occurred with that of $-61°$. From this decrease a relaxation time of approx. 130 ps was determined.

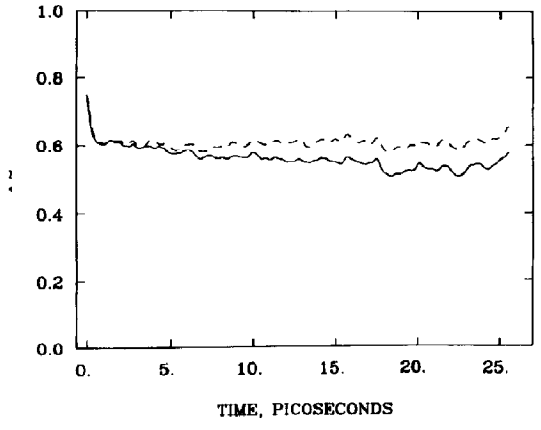

Fig. 5. Correlation function P_2 using a $\hat{\mu}_a(0)$ of $-38°$ and $\hat{\mu}_e(t)$ of $-15°$ (---) and $-61°$ (———) from free enzyme simulation.

4. Discussion

4.1. Fluorescence decay times

The presence of two or more fluorescence decay times in all three enzyme forms (table 1) indicates the presence of multiple conformations which may be related to the rotational motion being observed. The cause of the different lifetimes may be attributed to varied quenching of Trp 59 in the different enzyme conformations [21,22]. Such quenching, considering the inaccessibility of solvent to the tryptophan, is apparently due to an intrinsic protein group situated close to the Nε1 atom on the Trp 59 side chain [47]. Analysis of both the X-ray and molecular dynamics averaged structures suggests the peptide bond between Pro 60 and Ile 61 to be the quenching group. Thus, changes in the relationship between the Nε1 atom and the peptide bond in different enzyme conformations lead to the different decay times.

The relationship of the fluorescence decay times (table 1) to the measured Trp 59 motion may be modeled as follows. The measured Trp 59 motion is associated with the slower fluorescence decay times τ_3 and τ_4, because the fast fluorescence decay times, τ_1 and τ_2, observed in the enzyme-inhibitor complexes are so short compared to the fast rotational relaxation time, θ_2, that any contribution from those fast-decaying states to the measured Trp 59 internal motion is negligible. Com-

parison of the free enzyme and 3′-GMP-enzyme τ_3 and τ_4 fluorescence decay times and weights (table 1) shows good agreement in relation to the 2′-GMP-enzyme, supporting the conformational similarity of the free and 3′-GMP-enzyme forms (see below). The multiple fluorescence decays, rather than indicating discrete enzyme conformations, may also represent average values from a distribution of lifetimes [52] representative of various conformational substates of Trp 59 and its surrounding environment.

4.2. RNase T_1 conformation

X-ray crystallographic studies have been performed on the 2′-GMP- [32,33] and 3′-GMP- [34] enzyme complexes but not on the free enzyme. These studies have shown the two inhibitor-bound structures to be quite similar although some differences do occur in both the backbone atoms and inhibitor-enzyme contacts [34]. Differences in the backbone occur primarily in the loop regions, including part of the region surrounding Trp 59. Interactions between the inhibitors and the enzyme are similar around the guanosine bases [32–34,53], but some differences do occur around the ribose phosphate moieties. In the 2′-GMP-enzyme there are several hydrogen bonds between the phosphate and the enzyme, which appear to be pH dependent [32,33] as shown after the refinement of the models at high resolution (1.85 Å), although they are more closely related than previously thought (Arni et al., manuscript in preparation). The phosphate-enzyme hydrogen bonds involve residues Glu 58 (indicating that residue to be protonated at both pH 4.0 and 5.3), Tyr 38, His 40 (pH 5.3) and Arg 77 (pH 4.0). With the 3′-GMP-enzyme, however, no interpretable electron density at the present resolution is observed for the ribose-phosphate moiety [34], indicating that portion of the inhibitor to be in a highly disordered state, possibly existing in a variety of substates [12,15,54].

To understand better the differences between the enzyme conformations in the free enzyme, 2′-GMP-enzyme and 3′-GMP-enzyme [38], time-resolved fluorescence measurements were made at various temperatures on the three enzyme forms. Initial experiments in aqueous solution (fig. 1, table 2) indicated the free enzyme and 2′-GMP-enzyme forms to be more similar as compared to the 3′-GMP-enzyme. Results from the temperature effects in aqueous solution must be interpreted with caution, due to the measured activation parameters containing contributions from both the protein and the surrounding solvent (see above). To observe barriers in the protein alone experiments were next performed by maintaining viscosity while varying temperature (isoviscosity). The results from the isoviscosity experiment (fig. 2, table 3) indicated the free enzyme and 3′-GMP-enzyme forms to be more similar as compared to the 2′-GMP-enzyme form. Thus, from the experiment designed to observe activation barriers in the protein alone, the free enzyme and 3′-GMP-enzyme conformations, although somewhat different as demonstrated by the fluorescence decay times and rotational relaxation times (table 1) [38], appear to be similar while the 2′-GMP-enzyme conformation is significantly different.

Intuitively, results obtained for the protein alone seem reasonable. On a speculative basis, consider the three enzyme forms studied to be analogous to enzyme intermediates in the catalytic mechanism of RNase T_1; the free enzyme, the 2′-GMP-enzyme which is analogous to the cyclic 2′,3′-phosphate intermediate and the 3′-GMP-enzyme which is analogous to the enzyme-product complex. Thus, the 3′-GMP-enzyme form, which has the product relatively weakly bound and is catalytically one step from the free enzyme, would be expected to resemble conformationally the free enzyme. On the other hand, in the 2′-GMP-enzyme complex the enzyme, being more influenced by the bound inhibitor as indicated by the higher association constant and the X-ray crystallographic results and being two catalytic steps from the free enzyme, should have a conformation less similar to the free enzyme.

4.3. Solvent viscosity energetic analysis

Differences in the activation energy parameters from the protein and solvent together (aqueous solution, table 2) and the protein alone (isoviscos-

Table 4

Energetic activation parameters for the tryptophan motion associated with solvent viscosity

Errors are of the order of 10%. Free energies are for 293 K.

	Free enzyme	2′-GMP-enzyme	3′-GMP-enzyme
Enthalpy (kJ mol^{-1})	0.0	13.0	−13.0
Entropy (J mol^{-1} K^{-1})	4.2	46.8	−40.1
Free energy (kJ mol^{-1})	−1.3	−0.7	−1.3

ity, table 3) indicate the importance of the solvent viscosity contribution to the activation energy barrier in aqueous solutions. To analyze more closely the solvent viscosity contribution we assume that the protein-solvent activation energy parameters, $P^{\neq}_{tot}$, are simply the sum [12,13,16] of the solvent viscosity, $P^{\neq s}$, and protein, $P^{\neq *}$, activation energy parameters such that:

$$P^{\neq s} = P^{\neq}_{tot} - P^{\neq *} \quad (17)$$

Energy parameters associated with the solvent viscosity were then determined using the values in tables 2 and 3. Results from this evaluation (table 4) show the energy contributions from the solvent viscosity to vary for the different enzyme forms in the enthalpic and entropic terms. In all three cases the free energy term, due to compensation between the enthalpic and entropic terms, is negligible. Although the solvent viscosity free energy contributions are similar and negligible with all three enzyme forms the significant differences between the enthalpic and entropic terms indicate that changes in the enzyme conformation may lead to changes in the influence of solvent viscosity on the protein matrix.

4.4. Kramers' approach

The approach of Kramers as applied to activation barriers in proteins was tested by determining the rotational relaxation time, θ_2, for Trp 59 for various viscosities (isothermal conditions). The results (see fig. 3) gave values of κ, the protein transmission factor, ranging from 0.08 to 0.31 (see section 3). These values are in the range of those previously reported by Frauenfelder and coworkers [12] for myoglobin and hemoglobin. To calculate the activation free energies using Kramers' approach we assume that the pre-exponential values ($\nu_o \nu'_o \rho/3$), listed following eq. 13, are constant and that the temperature is 293 K. Using these values activation free energies, $\Delta G^{\neq *}$, of 16.3, 16.7 and 16.7 kJ/mol for the free enzyme, 2′-GMP-enzyme and 3′-GMP-enzyme were calculated, respectively. Comparison of these values with the activation free energy values listed in table 3 shows a reasonable agreement indicating that the two approaches used to determine the protein activation free energies are compatible.

4.5. Trp 59 motion

Analysis of the Trp 59 motion first requires an understanding of the environment of the residue. Inspection of the 2′-GMP-enzyme structure at pH 5.3 [32] shows Trp 59 to be in a hydrophobic environment between the β-pleated sheet, the α-helix being completely surrounded by the protein matrix (see fig. 6). The region around Trp 59 includes the α-helix residues Ala 19, Ala 22 and Gly 23 and other residues including Pro 39, Pro 60, Tyr 68 and Phe 80. The hydrophobicity of the residues in the vicinity of Trp 59 is consistent with the blue fluorescence emission maximum of the enzyme occurring at 324 nm (results not shown)

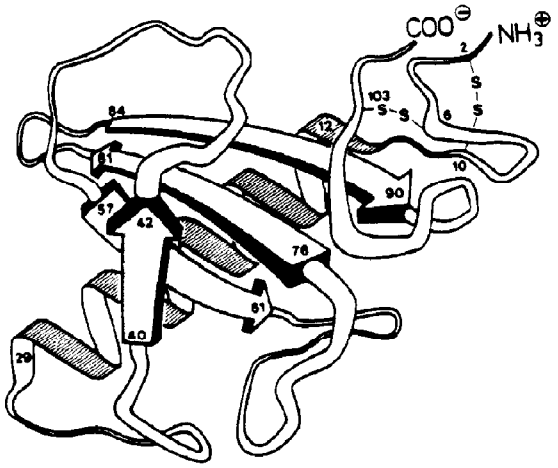

Fig. 6. Structure of ribonuclease T_1 in the presence of 2′-GMP (2′-GMP removed). From ref. 32.

[55–57]. Free space in the protein matrix around the residue is limited, indicating that a maximum rotation of the Trp 59 sidechain of approx. 10° could occur.

Results from the molecular dynamics simulation correlate well with the limited free space around Trp 59. In fig. 5 the correlation function P_2 between the Trp 59 absorption and emission vectors shows an initial very fast motion, which relaxes in about 1 ps, resulting in a decrease in r_o from 0.31 to 0.24. This decrease corresponds to an increase in the angle λ between the absorption and emission vectors of 8°, in good agreement with a 10° motion considering the free space around Trp 59. Furthermore, the molecular dynamics r_o value of 0.24 following the very fast motion agrees well with the experimentally measured $r_{o,total}$ of 0.26 (see section 3). Thus, it appears that Trp 59 vibrates quite rapidly within the available free space in the protein matrix. However, this very fast motion is beyond our current experimental resolution, indicating that the experimentally measured motion of 15–20° involves motion exceeding the available free space around Trp 59 and therefore requires a breathing of the surrounding protein matrix for that motion to occur.

Since the protein matrix must breathe in order for the Trp 59 motion to occur the fast rotational relaxation time, θ_2, being measured is directly related to the protein breathing rate. Considering that only the protein breathing can be measured we will present two preliminary models for the Trp 59 motion. The first model will assume that whenever the protein matrix, via the breathing motion, is shifted into the proper conformation motion of Trp 59 will occur. In this model the tryptophan will lie in one of two or more discrete enzyme conformations. It should be noted that these discrete conformations may each contain a variety of substates [4,15,54]. Such conformational substates may be responsible for the protein entropic terms (table 3) in the enzyme-inhibitor complexes. The second model represents a situation where Trp 59 moves in a correlated fashion with the breathing of the surrounding protein matrix leading to one broad distribution of conformational substates rather than two or more discrete conformations. In this model an opening of the protein matrix to allow Trp 59 to move never actually occurs, only a regional fluctuation of the protein matrix. The difference between the models is not the magnitudes of the measured rate constants but the 'allowed conformations' for Trp 59. In the first case Trp 59 is forced to jump between discrete wells and in the second Trp 59 is allowed to drift with the breathing of the protein matrix. These models, it should be emphasized, represent limiting cases whereas a realistic description of the system probably lies somewhere between the two.

Solvent viscosity contributions (table 4) to the overall activation energy parameters (aqueous solution, table 2) are much more significant in the enzyme-inhibitor complexes than in the free enzyme, indicating that the solvent viscosity effects are related to interactions within the enzyme's active site. These effects may be transmitted via Glu 58, among others, to the region of the enzyme containing Trp 59. Such transmission is probably aided by the presence of Glu 58 and Trp 59 on a β-strand associated with the β-pleated sheet in the enzyme. Furthermore, the presence of the highly conserved Pro 60 [58] confers further structural stability on the region containing amino acids 58–60. With the 2′-GMP-enzyme the enthalpic solvent viscosity term is unfavorable which may be associated with the hydrogen bonding in the region around the phosphate group of the bound inhibitor. The breaking of these bonds would then allow more conformational freedom (substates) which would account for the favorable entropic term. The situation in the 3′-GMP-enzyme is reversed, with a favorable solvent viscosity enthalpic term and an unfavorable entropic term (table 4). Here, the favorable enthalpic solvent viscosity term may indicate the requirement of a specific conformation or substate, requiring specific solvent-protein interactions, for the motion to occur. The specific solvent-protein configuration would be in contrast to the normal disordered state, as indicated by X-ray data [34], in the region of the bound 3′-GMP ribose phosphate moiety, and would simultaneously lead to a lower conformational freedom (number of substates) and hence to an unfavorable entropic term.

Values of κ from Kramers' approach (see above) indicate different transmission of solvent viscosity effects into the Trp 59 region between the free and 3′-GMP-enzyme forms vs. the 2′-GMP-enzyme. κ being lower for the free and 3′-GMP-enzyme forms indicates that solvent viscosity effects are transmitted less readily, which may be due to greater structural stability in the region around Trp 59 as shown by the higher protein enthalpic term (table 3). On the other hand, solvent viscosity effects in the active site may be more readily transmitted to the Trp 59 region in the 2′-GMP-enzyme due to a lower structural stability in that region, as indicated by the higher κ value and lower protein enthalpic term. Thus, with RNase T_1 it appears that the κ factor is inversely related to the protein enthalpic term. An apparent discrepancy still exists between the significant solvent viscosity energetic contributions for the 3′-GMP-enzyme (table 4) and the small value of κ as compared to the 2′-GMP-enzyme. A possible explanation may be that the actual solvent viscosity energetic contributions at the active site are much larger in the 3′-GMP-enzyme than with the 2′-GMP-enzyme. However, a greater damping effect by the protein matrix in the 3′-GMP-enzyme results in values similar in magnitude, albeit reversed, to those seen in the 2′-GMP-enzyme (table 4).

Molecular dynamics results, although somewhat preliminary on the time scale required to analyze effectively a motion of 100 ps, indicate the presence of a motion in the free enzyme on that time scale. Fig. 5, following the initial very fast motion, shows a gradual decay in the case of the $-61°$ emission vector which corresponds to a correlation time of approx. 130 ps. This result from the simulation at 324 K, considering the extreme extrapolation used to obtain it, agrees quite well with the measured rotational correlation time of approx. 100 ps for the free enzyme at 313 K (table 1). The hydrophobic environment of Trp 59, the low value of κ and the negligible solvent energetic terms in the free enzyme, all of which indicate a minimal influence of the solvent on the Trp 59 motion, are probably important for the good agreement between the experimental and vacuum simulation results.

Root mean square fluctuations of the residues in the free enzyme from the molecular dynamics simulation are presented in fig. 4. These results, which may act as a prediction for future results from X-ray temperature factors, further indicate the presence of motion of the Trp 59 side chain (fig. 4, top). Fluctuations of the α-helix residues 22 and 23 which lie directly adjacent to Trp 59 (fig. 6) are also significant and may contribute to the Trp 59 motion. Other residues of high mobility include the loops involving residues 43–50 and 93–96. Both of these regions are in the vicinity of the active site, towards the top of the enzyme in fig. 6, with the 43–50 residue loop interacting directly with the guanine base in the 2′-GMP-enzyme complex (refs. 32 and 33, revised model; Arni et al., manuscript in preparation). Fig. 4 also shows several regions of markedly low mobility, which correlate well with residues involved in the catalytic mechanism of RNase T_1 [37]. Analysis of the active-site region of the molecular dynamics averaged structure (results not shown) suggests the presence of a hydrogen-bonding network involving residues Glu 58, His 40, Arg 77 and Tyr 38. The structural stability of the active-site residues in this free enzyme structure may be responsible for the low solvent viscosity contribution to the activation parameters (see above, table 4) which are implicated as originating within the active site. Comparison of the high- and low-mobility regions in fig. 4 indicates that regions of the protein important for recognition of the guanine base are highly mobile, suggesting the mobility to be important for the primary recognition of the inhibitor by the enzyme, while the region including the catalytic residues that interact with the inhibitor phosphate are relatively immobile, possibly to allow for specific interactions required for further binding to occur.

Acknowledgements

This work was supported by a fellowship to A.D.M. from the Karolinska Institutet and grants from the Knut and Alice Wallenberg Foundation, the Swedish Natural Science Research Council, the Sonderforschungsbereich and by Fonds der Chemischen Industrie. We are grateful to Luit-

pold-Werke, Munich, for the free supply of Takadiastase from which the ribonuclease T_1 was isolated for use in these studies.

References

1 M. Karplus and J.A. McCammon, CRC Crit. Rev. Biochem. 9 (1981) 293.
2 J.A. McCammon, Rep. Prog. Phys. 47 (1984) 1.
3 A. Warshel, Proc. Natl. Acad. Sci. U.S.A. 81 (1984) 444.
4 H. Frauenfelder, G.A. Petsko and D. Tsernoglou, Nature 280 (1979) 558.
5 P.J. Artymiuk, C.C.F. Blake, D.E.P. Grace, S.J. Oatley, .C. Phillips and M.J.E. Sternberg, Nature 280 (1979) 563.
6 R. Richarz, K. Nahayama and K. Wuthrich, Biochemistry 19 (1980) 5189.
7 G. Lipari and A. Szabo, J. Am. Chem. Soc. 104 (1982) 4546.
8 G. Lipari and A. Szabo, J. Am. Chem. Soc. 104 (1982) 4559.
9 I. Munro, I. Pecht and L. Stryer, Proc. Natl. Acad. Sci. U.S.A. 76 (1979) 56.
10 G.S. Beddard and C.D. Tran, Eur. J. Biophys. 11 (1985) 243.
11 J.W. Petrich, J.W. Longworth and G.R. Fleming, in: Ultrafast phenomena V', eds. G.R. Fleming and A.E. Siegman, Springer Series in Chemical Physics, vol. 46 (Springer-Verlag, Berlin, 1986) p. 413.
12 D. Beece, L. Eisenstein, H. Frauenfelder, D. Good, M.C. Marden, L. Reinisch, A.H. Reynolds and L.B. Sorensen Biochemistry 19 (1980) 5147.
13 H. Frauenfelder and P.G. Wolynes, Science 229 (1985) 337.
14 H.A. Kramers, Physica 7 (1940) 284.
15 R.H. Austin, K.W. Beeson, L. Eisenstein, H. Frauenfelder and I.C. Gunsalus, Biochemistry 14 (1975) 5355.
16 B. Gavish and M.M. Werber, Biochemistry 18 (1979) 1269.
17 J.M. Beecham and L. Brand, Annu. Rev. Biochem. 54 (1985) 43.
18 R. Rigler, F. Claesens and G. Lomakka, in: Ultra-fast phenomena IV, eds. D.H. Auston and K.B. Eisenthal (Springer-Verlag, Heidelberg, 1984) p. 472.
19 R. Rigler, F. Claesens and O. Kristensen, Anal. Instrum. 14 (1985) 525.
20 R.M. Levy and A. Szabo, J. Am. Chem. Soc. 104 (1982) 2073.
21 M.C. Chang, J.Q. Petrich, D.B. McDonald and G.R. Fleming, J. Am. Chem. Soc. 105 (1983) 3819.
22 J.W. Petrich, D.B. Chang, D.B. McDonald and G.R. Fleming, J. Am. Chem. Soc. 105 (1983) 3824.
23 M.R. Eftink and C.A. Ghiron, Proc. Natl. Acad. Sci. U.S.A. 9 (1975) 3290.
24 A. Grinvald and I.Z. Steinberg, Biochim. Biophys. Acta 427 (1976) 663.
25 M.R. Eftink, Biophys. J. 43 (1983) 323.
26 J.R. Lakowicz, B.P. Maliwal, H. Cherek and A. Balter, Biochemistry 22 (1983) 1741.
27 D.R. James, D.R. Demmer, R.P. Steer and R.E. Verrall, Biocheminstry 24 (1985) 5517.
28 R.M. Levy, R.P. Sheridan, J.W. Keepers, G.S. Dubey, S. Swaminathan and M. Karplus, Biophys. J. 48 (1985) 509.
29 J.A. McCammon, P.G. Wolynes and M. Karplus, Biochemistry 18 (1979) 927.
30 J.A. McCammon and M. Karplus, Biopolymers 19 (1980) 1375.
31 T. Ichiye and M. Karplus, Biochemistry 22 (1983) 2884.
32 U. Heinemann and W. Saenger, Nature 299 (1982) 27.
33 S. Sugio, T. Anisak, H. Ohishi, K.I. Tomita, U. Heinemann and W. Saenger, FEBS Lett. 181 (1985) 129.
34 S. Sugio, T. Anisak, H. Ohishi, K.I. Tomita and W. Saenger, FEBS Lett. 183 (1985) 115.
35 F. Egami, K. Takahashi and T. Uchida, Prog. Nucleic Acid Res. Mol. Biol. 3 (1964) 59.
36 T. Uchida and F. Egami, The enzymes, vol. 4 (Academic Press, New York, 1971) p. 205.
37 K. Takahashi and S. Moore, The enzymes, vol. 13 (Academic Press, New York, 1982) p. 435.
38 A.D. MacKerell, Jr, R. Rigler, U. Hahn and W. Saenger, in: Structure, dynamics and function of biomolecules, eds. A. Ehrenberg, R. Rigler, A. Gräslund and L. Nilsson, Springer Series in Biophysics, vol. 1 (Springer-Verlag, Berlin, 1987) p. 260.
39 A. Rüterjans and O. Pongs, Eur. J. Biochem. 18 (1971) 313.
40 J.B. Seger, in: Glycerol, eds. C.S. Miner and N.N. Dalton (Reinhold, New York, 1953) p. 238.
41 R. Rigler and M. Ehrenberg, Q. Rev. Biophy. 9 (1976) 1.
42 F. Claesens and R. Rigler, Eur. J. Biophys. 13 (1986) 331.
43 A. Grinvald and I.Z. Steinberg, Anal. Biochem. 59 (1974) 583.
44 R. Rigler and M. Ehrenberg, Q. Rev. Biophys. 6 (1973) 139.
45 A.J. Cross, D.H. Waldeck and G.R. Fleming, J. Chem. Phys. 78 (1983) 6455.
46 A. Szabo, J. Chem. Phys. 81 (1984) 150.
47 L.S. Chen, J.W. Longworth and G.R. Fleming, Biophys. J. (1987) submitted for publication.
48 B. Brooks, R. Bruccoleri, B. Olafson, D.J. States, S. Swaminathan and M. Karplus, J. Comp. Chem. 4 (1983) 187.
49 A.G. Marshall, in: Biophysical chemistry (John-Wiley and Sons, Chichester, 1978) p. 105.
50 B. Valeur and G. Weber, Photochem. Photobiol. 25 (1977) 441.
51 Y. Yamamoto and J. Tanaka, Bull. Chem. Soc. Jap. 45 (1972) 1362.
52 E. Gratton, J.R. Alcala, G. Marriott and F.J. Prendergast, in: Structure, dynamics and function of biomolecules, eds. A. Ehrenberg, R. Rigler, A. Gräslund and L. Nilsson, Springer Series in Biophysics, vol. 1 (Springer-Verlag, Berlin, 1987) p. 132.
53 F. Inagaki, I. Shimada and T. Miyazawa, Biochemistry 24 (1985) 1013.
54 H. Frauenfelder, in: Structure, dynamics and function of biomolecules, eds. A. Ehrenberg, R. Rigler, A. Gräslund and L. Nilsson, Springer Series in Biophysics, vol. 1 (Springer-Verlag, Berlin, 1987) p. 10.

55 O. Pongs, Biochemistry 9 (1970) 2316.
56 D. Creed, Photochem. Photobiol. 39 (1984) 537.
57 R. Lumry and M. Hershberger, Photochem. Photobiol. 27 (1978) 819.
58 C. Hill, G. Dodson, U. Heinemann, W. Saenger, Y. Mitsui, K. Nakamura, S. Borisou, G. Tischenko, K. Polyakov and S. Pavlosvky, Trends Biochem. Sci. 8 (1983) 364.